



# A Car-Following Model Considering the Next-Nearest-Neighbor Interaction of Electronic Throttle Information

Yirong Kang<sup>1</sup>(✉) and Shuhong Yang<sup>2</sup>

<sup>1</sup> School of Transportation Engineering, Guizhou Institute of Technology,  
Guiyang 550003, China  
kyr6700256@126.com

<sup>2</sup> School of Computer Science and Communication, Guangxi  
University of Science and Technology, Liuzhou 545006, China

**Abstract.** Aiming at the problem that the nearest preceding car of the considered vehicle may leave the current lane and cause the latter to lose track reference, based on the classical FVD model, this paper design a more effective feedback control signal by considering the ET opening angle difference information from the next-nearest-neighbor interaction at the previous moment, and propose a new CAV cooperative driving following model. The effect of this new consideration upon the stability of CAV traffic flow is examined through linear stability analysis. A modified Korteweg-de Vries (mKdV) equation was derived via nonlinear analysis to describe the propagating behavior of traffic density wave near the critical point. Good agreement between the simulation and the analytical results shows that taking the next-nearest-neighbor interaction of electronic throttle historical information into account leads to the stabilization of traffic systems, and thus can efficiently suppress the emergence of traffic jamming. The results can be expected to provide a theoretical reference for designing more effective traffic congestion control strategies.

**Keywords:** Car-following Model · Electronic Throttle · Next-nearest-neighbor Interaction · Connected and Autonomous Vehicle

## 1 Introduction

With the fast growth of the economy and the pace of social development, the problem of traffic congestion is becoming increasingly prominent, which seriously hinders people's daily work and life. Studying on alleviating traffic congestion has attracted extensive attention, and many traffic flow models [1–5] have been proposed to provide theoretical support for solving traffic problems. At present, the existing traffic flow models can be roughly divided into three categories: macroscopic models, microscopic models, and mesoscopic models. The car-following model is a favorable type of microscopic traffic models, which describe the interaction between each pair of leading and following vehicles in the same lane based on the formula of stimulus response framework.

Among them, the most well-known one is the optimal velocity (OV) model proposed by Bando et al. [4], which has successfully revealed the dynamical evolution process of traffic congestion in a simple way. Hereafter, various OV-based car-following models have been proposed one after another by introducing actual traffic factors, such as multiple information of headway [5] or relative velocity [6], backward-looking effect [7], driver's anticipation [8], curved road condition [9] and so on. These car-following models mentioned above can reproduce complex traffic phenomena and reveal mechanism of traffic jams at a higher level.

Recently, along with the Vehicle-Vehicle communication technology, modeling the car following process of Connected and Autonomous Vehicle (CAV) has attracted increasing attention in the field of traffic flow. In this direction, some scholars successively developed some extended car following model by factoring the effect of electronic throttle (ET) opening angle. In 2016, based on the full velocity difference (FVD) model, Li et al. [10] proposed a throttle-based car following model (recorded as T-FVD) to describe the effect of ET opening angle on CAV traffic flow. After that, considering the factors of lateral gap and electronic throttle opening angle in the same time, they presented an extended car-following model under connected environment in 2017 [11]. Their results show that the stability of traffic flow with CAV is improved by introducing the new consideration. By making full use of ET angle control signal of multiple preceding vehicles, a novel car-following model was established with consideration of optimal velocity difference and ET angle information, in which the time-dependent Ginzburg-Landau (TDGL) equation and the modified Korteweg-de Vries (mKdV) equation are inferred to describe the evolutionary process of density wave [12]. In 2019, Sun et al. proposed an extended car-following model by taking the effect of ET signal into account on the curved road [13], in which the ET opening angle difference from multiple preceding vehicles at the previous moment is considered as a delay-feedback control signal.

A series of research results of CAV car-following model mentioned above demonstrate that with the help of vehicle-vehicle communication technology, the traffic jams can be effectively suppressed by exchanging the ET opening angle data among continuous preceding vehicles. However, the existing CAV car-following models are unsuited to study the ET opening angle influence of the next-nearest-neighbor interaction (non-adjacent the current vehicle), since they do not consider this factor at all. In fact, classic traffic flow research results [14, 15] have proved that the next-nearest-neighbor interaction factors have an important influence on car following scene. Naturally, there is an open question regarding to whether or not the next-nearest-neighbor interaction in electronic throttle dynamics affects the CAV car-following. However, to our knowledge, this open question has not been explored in the CAV car-following model up to now. In view of the above reason, in this paper, a new car-following model is constructed by considering the effect of ET dynamics for CAV traffic flow, in which the ET opening angle difference from the next-nearest-neighbor interaction at the previous moment is considered in the vehicle networking environment. The analytical and numerical simulation are conducted to show that the new consideration has significant influence on the stability and dynamic characteristics of CAV traffic flow.

## 2 Models

In 1995, Bando et al. proposed the OV model [4] to describe car-following behavior on a single-lane highway. The motion equation is as follows:

$$\frac{dv_j(t)}{dt} = a[V(\Delta x_j(t)) - v_j(t)] \quad (1)$$

where  $x_j(t)$  and  $v_j(t)$  are the position and velocity of the  $j$ th car respectively, and  $t$  represents time.  $a$  denotes the sensitivity of the driver and is given by the inverse of the delay time  $\tau$ , namely  $a = 1/\tau$ .  $\Delta x_j(t) = x_{j+1}(t) - x_j(t)$ , represents the headway of two successive vehicles.  $V(\cdot)$  is the optimal velocity function. Comparison with empirical data shows that too high acceleration and unrealistic deceleration occurs in OV model.

To overcome the deficiency of OV model, Helbing and Tilch [16] proposed a generalized force (GF) model via introducing a negative velocity difference into the OV model. Later, considering the positive relative velocity into the GF model, Jiang et al. [17] developed the full velocity difference (FVD) model as follows:

$$\frac{dv_j(t)}{dt} = a[V(\Delta x_j(t)) - v_j(t)] + \lambda \Delta v_j(t) \quad (2)$$

where  $\Delta v_j(t) = v_{j+1}(t) - v_j(t)$  is the velocity difference between the leading car  $j + 1$  and the following car  $j$  at time  $t$ .  $\lambda$  is the responding factor of the velocity difference. The results illustrate that the FVD model has better agreement with field data, compared with the OV and GF models. However, unrealistically high deceleration also occurs in the FVD model [17].

To capture the nature of CAV traffic flow, Li et al. [10] proposed the throttle-based FVD (T-FVD) model by introducing the effect of ET opening angle into the FVD model. The dynamic equation is described as follows:

$$\frac{dv_j(t)}{dt} = a[V(\Delta x_j(t)) - v_j(t)] + \lambda \Delta v_j(t) + \gamma \Delta \theta_j(t) \quad (3)$$

where  $\theta_j(t)$  is the electronic throttle opening angle of  $j$ th vehicle at time  $t$ .  $\Delta \theta_j(t) = \theta_{j+1}(t) - \theta_j(t)$  represents the ET opening angle difference between the vehicle  $j + 1$  and the vehicle  $j$  at time  $t$ .  $\gamma > 0$  is the control coefficient of the angle difference.

According to the existing literature [10, 12], the mathematical relationship between the electronic throttle angle and the velocity difference and acceleration can be expressed as follows.

$$\frac{dv_j(t)}{dt} = -p(v_j(t) - v_e) + q(\theta_j(t) - \theta_e) \quad (4)$$

where  $p$  and  $q$  are constant greater than zero,  $v_e$  is the current equilibrium speed,  $\theta_e$  is the electronic throttle angle, it corresponds to the current equilibrium speed.

According to the idea mentioned in the introduction, this paper proposes an extended model by considering the information of the ET opening angle difference from the next-nearest-neighbor interaction at the previous moment. The proposed model is represented as follows:

$$\frac{dv_j(t)}{dt} = a[V(\Delta x_j(t)) - v_j(t)] + \lambda \Delta v_j(t) + k[\theta_{j+2}(t-1) - \theta_{j+1}(t-1)] \quad (5)$$

where the next-nearest-neighbor interaction term  $\theta_{j+2}(t-1) - \theta_{j+1}(t-1)$  is the historical information of ET opening angle difference between the  $(j+2)$ th vehicle and its following vehicle  $(j+1)$ th at time  $t-1$ .  $k$  is the sensitivity coefficient. The control strategy of this extended CAV car following model is that the host car adjusts his acceleration not only by the received information of velocity  $v_j(t)$  and velocity difference  $\Delta v_j(t)$  of the  $j$ th car at time  $t$ , but also by the collected signal of ET opening angle difference  $\theta_{j+2}(t-1) - \theta_{j+1}(t-1)$  from the next-nearest-neighbor interaction at the previous moment  $t-1$ . When  $k=0$ , the new model degenerates into FVD model [17].

According to Eq. (4), we can get

$$\theta_j(t) = \frac{1}{q} \left[ \frac{dv_j(t)}{dt} + p(v_j(t) - v_e) \right] + \theta_e \quad (6)$$

Thus, we can obtain the opening angle difference of electronic throttle between the  $(n+2)$ th and the  $(n+1)$ th vehicles at time  $t-1$  as

$$\begin{aligned} \theta_{j+2}(t-1) - \theta_{j+1}(t-1) &= \frac{1}{q} \left[ \frac{dv_{j+2}(t-1)}{dt} - \frac{dv_{j+1}(t-1)}{dt} \right. \\ &\quad \left. + p(v_{j+2}(t-1) - v_{j+1}(t-1)) \right] \end{aligned} \quad (7)$$

Substituting Eq. (7) into Eq. (5), we can rewrite Eq. (5) as:

$$\begin{aligned} \frac{dv_j(t)}{dt} &= a[V(\Delta x_j(t)) - v_j(t)] + \lambda \Delta v_j(t) \\ &+ k \cdot \frac{1}{q} \left[ \frac{dv_{j+2}(t-1)}{dt} - \frac{dv_{j+1}(t-1)}{dt} + p(v_{j+2}(t-1) - v_{j+1}(t-1)) \right] \end{aligned} \quad (8)$$

For the convenience of nonlinear analysis, Eq. (8) can be further rewritten as:

$$\begin{aligned} \frac{d^2 \Delta x_j(t)}{dt^2} &= a[V(\Delta x_{j+1}(t)) - V(\Delta x_j(t)) - \frac{d \Delta x_j(t)}{dt}] + \lambda \left[ \frac{d \Delta x_{j+1}(t)}{dt} - \frac{d \Delta x_j(t)}{dt} \right] \\ &+ k \cdot \frac{1}{q} \left\{ \frac{d^2 \Delta x_{j+2}(t-1)}{dt^2} - \frac{d^2 \Delta x_{j+1}(t-1)}{dt^2} + p \left[ \frac{d \Delta x_{j+2}(t-1)}{dt} - \frac{d \Delta x_{j+1}(t-1)}{dt} \right] \right\} \end{aligned} \quad (9)$$

In this paper, we take the following optimal velocity function (for short, OVF) calibrated with the empirical data by Helbing [16]:

$$V(\Delta x_j) = V_1 + V_2 \tanh[C_1(\Delta x - l_c) - C_2] \quad (10)$$

Here, parameters in the OVF are set as  $a = 0.85 \text{ s}^{-1}$ ,  $V_1 = 6.75 \text{ m/s}$ ,  $C_2 = 1.57$ ,  $C_1 = 0.13 \text{ m}^{-1}$ ,  $V_2 = 7.91 \text{ m/s}$  and the length of the vehicle is  $l_c = 5 \text{ m}$ .

### 3 Linear Stability Analysis

There is no doubt that the performance of stability is the most important characteristic of CAV traffic flow control system. In this section, the linear stability analysis is conducted

to investigate the stabilizing ability of ET in CAV scene. It is obvious that the CAV traffic flow reach steady state when the cars run with the uniform headway  $b$  and optimal velocity  $V(b)$ . Therefore, the steady-state solution is given as,

$$x_j^0(t) = bj + V(b)t, b = L/N \tag{11}$$

where  $L$  is the road length and  $N$  is the total car number. Suppose  $y_j(t)$  is a small deviation from the steady state  $x_j^0(t)$ :  $x_j(t) = x_j^0(t) + y_j(t)$ . Substituting it into Eq. (8) and linearizing them yields

$$y_j''(t) = a[V'(b)\Delta y_j(t) - y_j'(t)] + \lambda[y_{j+1}'(t) - y_j'(t)] + k \cdot \frac{1}{q}\{y_{j+2}''(t-1) - y_{j+1}''(t-1) + p[y_{j+2}'(t-1) - y_{j+1}'(t-1)]\} \tag{12}$$

where  $V' = dV(\Delta x_j)/d\Delta x_j|_{\Delta x_j=b}$  And  $\Delta y_j(t) \equiv y_{j+1} - y_j$ .

Via expanding  $y_j(t) = Ae^{ikj+zt}$ , where  $z = z_1(ik) + z_2(ik)^2 + \dots$ , and inserting them into Eq. (12). One has the first- and second-order terms of  $ik$  respectively,

$$z_1 = V'(b), z_2 = \frac{1}{2}V'(b) + (\frac{\lambda}{a} + \frac{1}{aq}kp)V'(b) - \frac{1}{a}[V'(b)]^2 \tag{13}$$

If  $z_2 < 0$ , the uniformly steady-state flow becomes unstable, while the uniform flow is stable when  $z_2 > 0$ . Thus the neutral stable criteria for this steady state is given by

$$a = 2[V'(b) - \lambda - \frac{1}{q}kp] \tag{14}$$

For small disturbance with long wavelengths, the homogeneous traffic flow is stable in the condition that

$$a > 2[V'(b) - \lambda - \frac{1}{q}kp] \tag{15}$$

As  $k = 0$ , the result of stable condition is the same as that of the FVD model [17].

$$a > 2[V'(b) - \lambda] \tag{16}$$

The neutral stable condition Eq. (14) clearly show that the sensitivity coefficient  $k$  play an important role in stabilizing the CAV traffic flow. The neutral stable curves under different values of  $k$  are depicted in the headway-sensitivity space  $(\Delta x, a)$  for the proposed model with  $p = 0.8, q = 0.27, \lambda = 0.3$ . In Fig. 1, the headway-sensitivity space is divided into two different parts by each curve. The upper part of neutral stability line denotes the stable area, and the lower part of the curve represents unstable area. Different regions mean that traffic flow of CAV will show different evolution states when small disturbances are added. Generally, when the traffic flow is in a stable area, the small disturbances will eventually evolve into a uniform state of motion. However, when it is in an unstable state, the unstable signal will be gradually enlarged, and the corresponding traffic flow will eventually evolve into a congestion state with time. From Fig. 1, one can see that every curve exists apex  $(h_c, a_c)$  named critical point. As  $k$  increases, the unstable region is compressed gradually, and the corresponding critical point of each curve decreases gradually, which means that the new consideration leads to the stabilization of CAV traffic systems. Particularly, as  $k = 0$ , the neutral stability line is the same as that of FVD model [17].

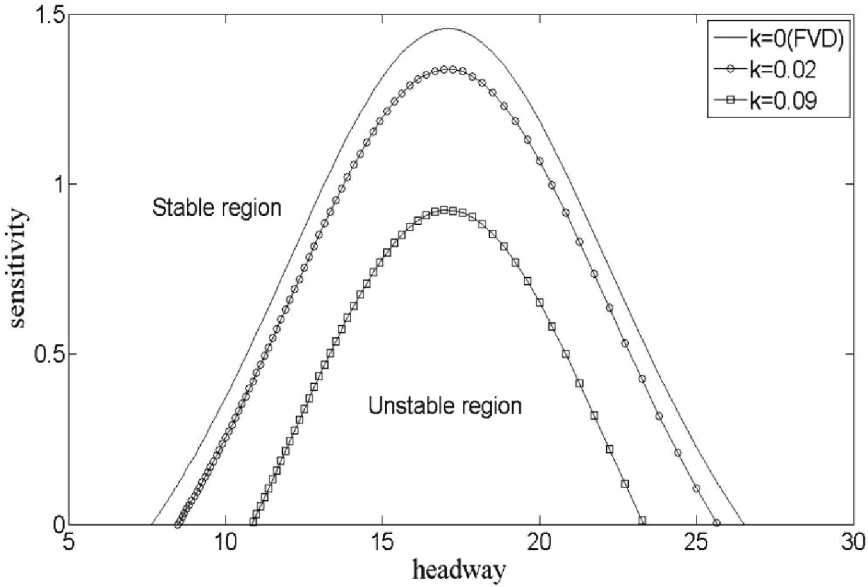


Fig. 1. The neutral stability curves in headway-sensitivity space  $(\Delta x, a)$

### 4 Nonlinear Analysis and mKdV Equation

To investigate the slowly varying behavior of CAV traffic flow near the critical point  $(h_c, a_c)$ , nonlinear analysis and derivation of the mKdV density wave equation are conducted to describe traffic jam propagation near critical point. For extracting slow scales with the space variable  $j$  and the time variable  $t$ , the slow variable  $X$  and  $T$  are defined as follows:

$$\begin{aligned} X &= \varepsilon(j + bt) \text{ and} \\ T &= \varepsilon^3 t, 0 < \varepsilon \leq 1 \end{aligned} \tag{17}$$

where  $b$  is a constant to be determined. Given

$$\Delta x_j(t) = h_c + \varepsilon R(X, T) \tag{18}$$

Substituting Eq. (17) and Eq. (18) into Eq. (9) and making the Taylor expansion to the fifth order of  $\varepsilon$  lead to the following expression:

$$\begin{aligned} &\varepsilon^2(b - V')\partial_X R + \varepsilon^3\left(\frac{b^2}{a} - \frac{V'}{2} - \frac{\lambda b}{a} - \frac{1}{aq}kpb\right)\partial_X^2 R + \varepsilon^4\left\{\partial_T R - \left[\frac{V'}{6} + \frac{b\lambda}{2a}\right.\right. \\ &+ \left.\left.\frac{2kb^2 + kpb(3 - 2b)}{2aq}\right]\partial_X^3 R - \frac{1}{6}V'''\partial_X R^3\right\} + \varepsilon^5\left\{\left(\frac{2b}{a} - \frac{\lambda}{a} - \frac{1}{aq}kp\right)\partial_T \partial_X R \right. \\ &\left. - \left[\frac{V'}{24} + \frac{\lambda b}{6a} + \frac{3kb^2(3 - 2b) + kpb(3b^2 - 9b + 7)}{6aq}\right]\partial_X^4 R - \frac{1}{12}V'''\partial_X^2 R^3\right\} = 0 \end{aligned} \tag{19}$$

where  $V' = [dV(\Delta x_j)/d\Delta x_j]|_{\Delta x_j=h_c}$  and  $V''' = [d^3V(\Delta x_j)/d\Delta x_j^3]|_{\Delta x_j=h_c}$ .

Near the critical point  $(h_c, a_c)$ ,  $\tau = (1 + \varepsilon^2)\tau_c$ , taking  $b = V'$  and eliminating the second order and third order terms of  $\varepsilon$  from Eq. (19) result in the simplified equation:

$$\varepsilon^4[\partial_T R - g_1 \partial_X^3 R + g_2 \partial_X R^3] + \varepsilon^5[g_3 \partial_X^2 R + g_4 \partial_X^4 R + g_5 \partial_X^2 R^3] = 0 \quad (20)$$

where

$$g_1 = \frac{V'}{6} + \frac{b\lambda\tau_c}{2} + \frac{2kb^2 + kpb(3-2b)}{2q}\tau_c \quad (21)$$

$$g_2 = -\frac{V'''}{6}g_2 = -\frac{V'''}{6} \quad (22)$$

$$g_3 = (b - \lambda - \frac{1}{q}kp)b\tau_c \quad (23)$$

$$g_4 = (2b - \lambda - \frac{1}{q}kp)\tau_c[\frac{V'}{6} + \frac{b\lambda\tau_c}{2} + \frac{2kb^2 + kpb(3-2b)}{2q}\tau_c] \\ - [\frac{V'}{24} + \frac{\lambda b\tau_c}{6} + \frac{3kb^2(3-2b) + kpb(3b^2 - 9b + 7)}{6q}\tau_c] \quad (24)$$

$$g_5 = \frac{1}{12}[(4b - 2\lambda - \frac{2}{q}kp)\tau_c - 1]V''' \quad (25)$$

To derive the regularized equation, the following transformations are performed on Eq. (20):

$$T' = g_1 T, \quad R = \sqrt{\frac{g_1}{g_2}} R' \quad (26)$$

The standard mKdV equation with a  $O(\varepsilon)$  correction term is given as follows:

$$\partial_{T'} R' - \partial_X^3 R' + \partial_X R'^3 + \varepsilon M[R'] = 0 \quad (27)$$

where

$$M[R'] = \sqrt{\frac{1}{g_1}}[g_3 \partial_X^2 R' + g_4 \partial_X^4 R' + \frac{g_1 g_5}{g_2} \partial_X^2 R'^3] \quad (28)$$

Ignoring the  $O(\varepsilon)$  term, we can obtain the mKdV equation with the kink-antikink soliton solution:

$$R'_0(X, T') = \sqrt{c} \tanh \sqrt{\frac{c}{2}}(X - cT') \quad (29)$$

With the method described in Ref. [18], we obtain the selected velocity  $c$ .

$$C = \frac{5g_2g_3}{2g_2g_4 - 3g_1g_5} \quad (30)$$

Hence, we obtain the kink-antikink soliton solution as follows:

$$\Delta x_j(t) = h_c + \sqrt{\frac{g_1 C}{g_2} \left(\frac{\tau}{\tau_c} - 1\right)} \tanh \sqrt{\frac{C}{2} \left(\frac{\tau}{\tau_c} - 1\right)} [j + (1 - C g_1 \left(\frac{\tau}{\tau_c} - 1\right))t] \quad (31)$$

Then, amplitude  $A$  of the kink-antikink soliton is given by

$$A = \sqrt{\frac{g_1 C}{g_2} \left(\frac{\tau}{\tau_c} - 1\right)} \quad (32)$$

The kink-antikink solution represents the coexisting phases, which consists of the freely moving phase at low density and the congestion jam at high density. Through nonlinear analysis, the propagating property of traffic jams near the critical point can be described by the solution of the mKdV density wave equation. Based on Eq. (30), the values of propagation velocity  $C$  under different values of  $k$  are shown in Table 1 for the proposed model. From Table 1, it can be found when  $k$  increases, the critical value  $a_c$  and the propagation speed  $C$  of traffic waves (jams) decrease gradually, which means that the stability of traffic flow increases gradually and the traffic jams has been reduced significantly by considering the effect of ET opening angle difference from the next-nearest-neighbor interaction at the previous moment. When  $k = 0$ , the result is the same as that in the FVD model [17].

**Table 1.** The critical sensitivity  $a_c$  and the propagation speed  $C$  for the proposed model when  $p = 0.8, q = 0.27, \lambda = 0.3$ .

$K$	0	0.02	0.04	0.06	0.08
$a_c$	1.4566	1.3973	1.3381	1.2788	1.2196
$C$	2.3376	1.7415	1.3288	1.0271	0.7977

## 5 Numerical Simulation and Validation

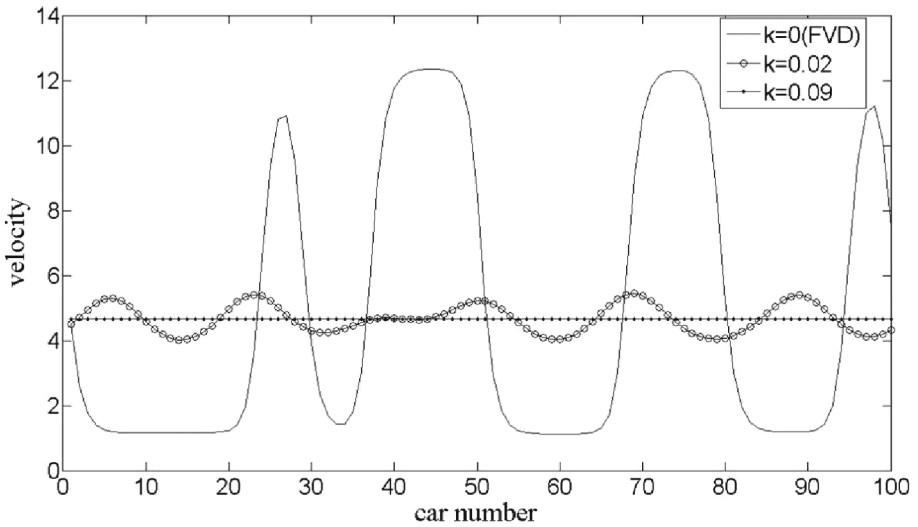
The numerical simulation is carried out under a periodic boundary condition to verify the effectiveness of theoretical analysis for the new model. The platform for all numerical simulation and validation is a computer with Intel Core(TM) i7 8700 CPU @ 3.2 GHz and 16G RAM. Matlab is employed as the programming language. The total car number  $N = 100$  and circuit length  $L = 1500$  m. The related parameters are taken as  $a = 1, p = 0.8, q = 0.27, \lambda = 0.3$ . The initial disturbance is same as that in Ref. [18]:

$$x_1(0) = 1 \text{ m}, x_1(0) = (n - 1)L/N \text{ m for, } n \neq 1 \quad (33)$$

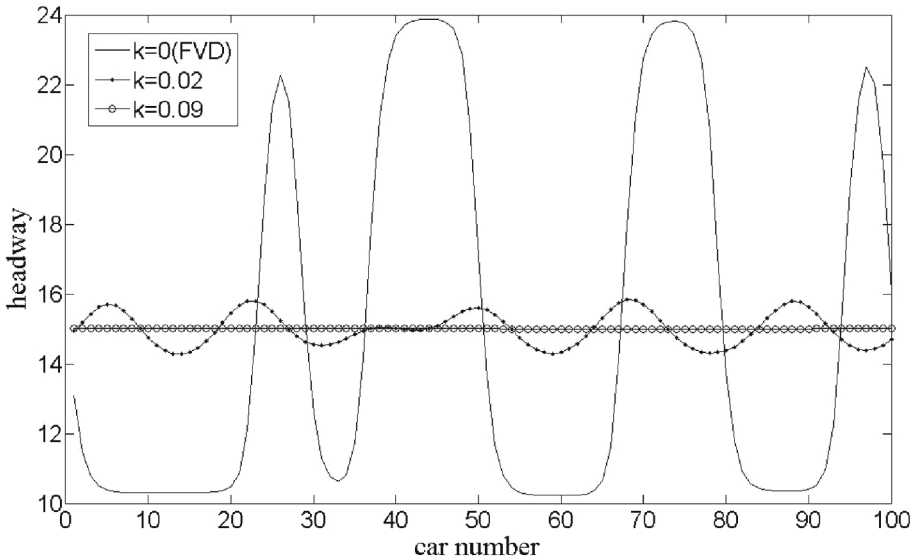
$$\dot{x}_n(0) = V(L/N) \text{ (} n = 1, 2, \dots, N \text{)} \quad (34)$$



Figures 2 and 3 demonstrate snapshots of all vehicles' velocity and headway at  $t = 1000s$  for different values of  $k$  respectively. When  $k = 0$ , the results are consistent with FVD model [17]. In Fig. 2 and 3, when  $k = 0$  and  $k = 0.02$ , the stability conditions are not satisfied, the initial disturbance propagates along the upstream of the CAV traffic flow and enlarges gradually, and finally evolves into a stop-and-go waves (traffic jams). However, under the same condition, because of the new consideration is introduced into the proposed model, one can observe clearly in Fig. 2 and Fig. 3 that the fluctuation amplitude of speed and headway of the new model are smaller than that of FVD model [17], which means that the stability is improved by incorporating the historical information of next-nearest-neighbor interaction of electronic throttle. Furthermore, with the increasing value of  $k$ , the number of stop-and-go waves and the corresponding fluctuation amplitude reduced obviously in the snapshot of velocity and headway, hence the system stability of CAV traffic flow is enhanced effectively. Especially, when  $k = 0.09$ , the stability condition hold true and thus the initial small disturbance signal will gradually decay, and the CAV traffic flow finally become stable again after a sufficiently long time.



**Fig. 2.** Snapshot of the velocities of all vehicles at different values  $k$  when  $t = 1000s$  in the new model ( $a = 1, p = 0.8, q = 0.27, \lambda = 0.3$ ).



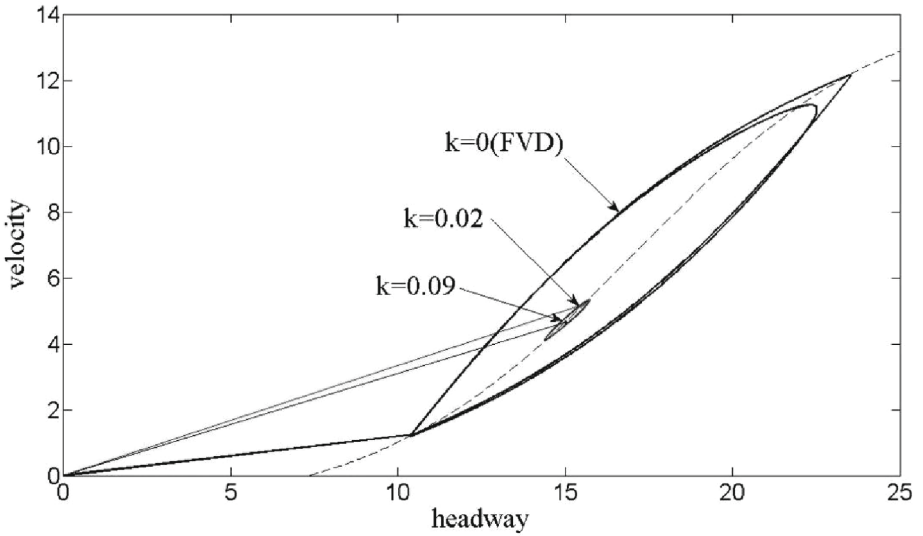
**Fig. 3.** Snapshot of the headway of all vehicles at different values  $k$  when  $t = 1000s$  in the new model ( $a = 1, p = 0.8, q = 0.27, \lambda = 0.3$ ).

Figure 4 shows the velocity-headway trajectory of the proposed model for different value of  $k$ . After sufficiently long time, the closed trajectories called hysteresis loops are clearly observed. In Fig. 4, as the value of  $k$  increases, the area of hysteresis loop becomes progressively smaller. This indicates that the new consideration plays a positive function on the stabilization of traffic flow. Particularly, when  $k = 0.09$ , the loop will shrink into a point on the optimal velocity curve, and the traffic flow get the stability state.

In order to investigate the performance of the proposed model further, we analyze the start-up velocity and delay time of vehicle queue compared with classical FVD model. The initial conditions and parameters are consistent with reference [17]: When  $t < 0$ , the signal light is red, the 11 cars are evenly lined up at intervals of 7.4 m, the corresponding speed is zero, and when  $t = 0$ , the signal light changes from red to green, all the cars began to speed up.

We define the delay time of car motion by  $\delta t$  as that in FVD model [17], Then the kinematic wave speed can be defined as  $c_j = 7.4/\delta t$ . The statistical results are shown Table 2 by taking the same parameters as those in FVD model [17].

As shown in Table 2, the velocity  $c_j$  of the proposed model are included in the expected range [17 km/h, 23 km/h] just as Bando et al. [4] pointed out, while the delay time  $\delta t$  is obviously shorter than FVD model. Which illustrates that by considering the ET opening angle difference information from the next-nearest-neighbor interaction at the previous moment, our model can respond to the change of preceding car more quickly, and thus is benefit to the smoothing of traffic.



**Fig. 4.** The loops for new model under different values  $k$ . The dashed curve represents OVf.

**Table 2.**  $\delta t$  and  $c_j$  in FVD model and the proposed model.

Model	$a(s^{-1})$	$\lambda(s^{-1})$	$k(s)$	$\delta t(s)$	$c_j(km/h)$
FVD	0.41	0.5	0	1.4	19.03
Our model	0.41	0.5	0.01	1.2	22.11

## 6 Conclusions

In this paper, a new car-following model is proposed by considering the information of next-nearest-neighbor interaction of electronic throttle at the previous moment for the connected Autonomous Vehicles environment. The influence of the electronic throttle information on the stability of CAV traffic flow is investigated by using the linear stability theory. Furthermore, on the basis of previous linear analysis, the mKdV equation has been derived to describe the density wave of CAV traffic flow near the critical point through nonlinear analysis. The simulation results are in good agreement with theoretical analysis and further indicate that, taking the historical information of next-nearest-neighbor interaction of electronic throttle into account, the traffic congestion can be effectively alleviated and the stabilization of CAV car following process can be achieved. Therefore, it is reasonable to conclude that historical information of the next-nearest-neighbor interaction of electronic throttle plays an important role in stabilizing the traffic flow in car following process and thus should be considered in traffic flow modeling.

**Acknowledgments.** This work is supported by Science and Technology Plan Projects of Guizhou Province: (No. 20181059) and Natural Science Foundation of Guangxi (No. 2018GXNS-FAA050020).

## References

1. Sun, B., Wu, N., Ge, Y.E., et al.: A new car following model considering acceleration of lead vehicle. *Transport* **31**(1), 1–10 (2016)
2. Zhang, Y., Ni, P., Li, M., et al.: A new car-following model considering driving characteristics and preceding vehicle's acceleration. *J. Adv. Transp.* 1–14 (2017)
3. Cao, B.G.: A car-following dynamic model with headway memory and evolution trend. *Physica A* **539**, 122903 (2020)
4. Bando, M., Hasebe, K., Nakayama, A., et al.: Dynamical model of traffic congestion and numerical simulation. *Phys. Rev. E* **51**(2), 1035 (1995)
5. Redhu, P., Siwach, V.: An extended lattice model accounting for traffic jerk. *Physica A* **492**, 1473–1480 (2018)
6. Ge, H.X., Cheng, R.J., Li, Z.P.: Two velocity difference model for a car following theory. *Physica A* **387**, 5239–5245 (2008)
7. Ge, H.X., Zhu, H.B., Dai, S.Q.: Effect of looking backward on traffic flow in a cooperative driving car following model. *Eur Phys J B* **54**, 503–507 (2006)
8. Tang, T.Q., Li, C.Y., Huang, H.J.: A new car-following model with the consideration of the driver's forecast effect. *Phys. Lett. A* **374**(38), 3951–3956 (2010)
9. Zhang, L.D., Jia, L. Zhu, W.X.: Curved road traffic flow car-following model and stability analysis. *Acta Phys. Sin.* **61**(7), 074501 (2012)
10. Li, Y.F., Zhang, L., Peeta, S., et al.: A car-following model considering the effect of electronic throttle opening angle under connected environment. *Nonlinear Dynam.* **85**, 2115–2125 (2016)
11. Li, Y.F., Zhao, H., Zheng, T.X., et al.: Non-lane-discipline-based car-following model incorporating the electronic throttle dynamics under connected environment. *Nonlinear Dynam.* **90**, 2345–2358 (2017)
12. Yan, C.Y., Ge, H.X., Cheng, R.J.: An extended car-following model by considering the optimal velocity difference and electronic throttle angle. *Physica A* **535**, 122216 (2019)
13. Sun, Y.Q., Ge, H.X., Cheng, R.J.: A car-following model considering the effect of electronic throttle opening angle over the curved road. *Physica A* **534**, 122377 (2019)
14. Nagatani, T.: Stabilization and enhancement of traffic flow by the next-nearest-neighbor interaction. *Phys. Rev. E* **60**(6), 6395–6401 (1999)
15. Li, Z.P., Liu, Y.C., Liu, F.Q.: A dynamical model with next-nearest-neighbor interaction in relative velocity. *Int. J. Mod. Phys. C* **18**(05), 819–832 (2011)
16. Helbing, D., Tilch, B.: Generalized force model of traffic dynamics. *Phys. Rev. E* **58**, 133–138 (1998)
17. Jiang, R., Wu, Q.S., Zhu, Z.J.: Full velocity difference model for a car-following theory. *Phys. Rev. E* **64**, 017101 (2001)
18. Ge, H.X., Cheng, R.J., Dai, S.Q.: KdV and Kink-Antikink solitons in car-following models. *Physica A* **357**(3–4), 466–476 (2005)